crystals

MDPI

*Article*

# Oxalate Crystallization under the Action of Brown Rot Fungi

**Dmitry Yu. Vlasov [1,2,*], Marina S. Zelenskaya [1], Alina R. Izatulina [3], Svetlana Yu. Janson [4] and Olga V. Frank-Kamenetskaya [3,*]**

[1] Department of Biology, St. Petersburg State University, University Emb. 7/9, 199034 St. Petersburg, Russia
[2] V.L. Komarov Botanical Research Institute, Russian Academy of Science, Prof. Popov Street 2, 197376 St. Petersburg, Russia
[3] Crystallography Department, Institute of Earth Sciences, St. Petersburg State University, 7/9, University Emb., 199034 St. Petersburg, Russia
[4] Microscopy and Microanalysis Resource Center, Research Park, St. Petersburg State University, University Emb. 7/9, 199034 St. Petersburg, Russia
* Correspondence: d.vlasov@spbu.ru (D.Y.V.); o.frank-kamenetskaia@spbu.ru (O.V.F.-K.)

**Abstract:** Brown rot fungi belong to the wood-rotting fungi, which produce oxalic acid and actively decompose wood. We first found oxalates formed under the action of brown rot fungi in natural conditions on stone (Rogoselga adit, Karelia, Russia), proposed a model for their formation, and confirmed the hypothesis that frequent occurrence of metal oxalates in mines and adits may be associated with the activity of these fungi. We synthesized under the action of four species of brown-rot fungi (*Serpula himantioides*, *Serpula lacrymans*, *Coniophora puteana*, *Antrodia xantha*) on different mineral substrates analogs of all known biofilm oxalate minerals and oxalates of such toxic heavy metals as Pb, Cu, Mn. In addition, we compared the features of oxalate formation under the action of brown rot fungi and soil fungus *Aspergillus niger*, an active oxalic acid producer, widely used in model experiments and recommended for application in biotechnologies. It is shown that in contrast to *A.niger*, the contribution of the metabolic activity of brown rot fungi to oxalate crystallization exceeds the contribution of the underlying minerals. The prospects for the use of brown rot fungi such as *Serpula himantioides*, *Coniophora puteana*, and *Antrodia xantha* in modern environmentally friendly biotechnologies are justified.

**Keywords:** microbial biomineralization; brown rot fungi; oxalates; toxic heavy metals; biotechnologies

check for updates

**Citation:** Vlasov, D.Y.; Zelenskaya, M.S.; Izatulina, A.R.; Janson, S.Y.; Frank-Kamenetskaya, O.V. Oxalate Crystallization under the Action of Brown Rot Fungi. *Crystals* **2023**, *13*, 432. https://doi.org/10.3390/cryst13030432

Academic Editors: Jaime Gómez Morales and Elena Sturm

Received: 13 February 2023
Revised: 23 February 2023
Accepted: 28 February 2023
Published: 2 March 2023

**Copyright:** © 2023 by the authors. Licensee MDPI, Basel, Switzerland. This article is an open access article distributed under the terms and conditions of the Creative Commons Attribution (CC BY) license (https://creativecommons.org/licenses/by/4.0/).

## 1. Introduction

Wood-rotting fungi are able to decompose wood in various environmental conditions. There are different mechanisms of wood decomposition associated with fungal biochemical characteristics, especially different enzyme compositions. Wood-rotting fungi produce a lot of oxalic acid that contributes to the decomposition of such wood components as lignin and cellulose [1–3].

A recent review article [4] reported that many wood-rotting fungi are able to reduce heavy metals in an environment (Pb, Cd, Co, Cr, Cu, Ni, Zn, Hg). The ability to produce a large amount of biomass as well as a significant amount of oxalic acid under control conditions makes wood-rotting fungi promising for use in bioremediation and other technologies [4–6].

There is no direct evidence that these fungi can live on stone but there are assumptions that they can move to rocks and minerals from wood. These proposals are based on the findings of metal oxalates in mines and adits [7–9].

Such assumptions are also supported by the results of numerous model experiments in which metal oxalates (Ca, Mn, Zn, Cu, Co, Pb, Cd) were obtained under the action of wood-rotting fungi on artificial and natural mineral substrates [5,6,10,11].

Wood-rooting fungi are divided into two large groups, white and brown rot fungi, based on the ability to decompose different components of wood, lignin and cellulose, respectively [1,2].

The objects of our research are brown rot fungi. They are also called house (domestic) fungi because of their capability to damage timber in buildings, engineering constructures, mines, and tunnels. It is well known that the cellulose component of wood is used actively by brown rot fungi as a source of nutrition. This contributes to a more intensive release of oxalic acid and the damage of wood. The formation of oxalic acid by these fungi is associated with its function of reducing Fe(III) to Fe(II) and its subsequent participation in the depolymerizing cellulose [2].

Known brown rot fungi of genera *Serpula*, *Coniophora*, and *Antrodia* are widespread in nature [12–14]. In laboratory conditions, they are able to form oxalates of some metals on various mineral substrates (Table 1). However, mainly calcium oxalates were synthesized in numerous experiments, while heavy metal oxalates (Pb, Cu, Mn) were received only in a few cases. In addition, there are no data on the synthesis of one of the biofilm minerals—magnesium oxalate glushinskite as well as iron oxalate humboldtine—the presence of which in biofilms is still questionable.

**Table 1.** Metal oxalates obtained in vitro under the action of brown rot fungi.

| Oxalates | Underlying Stone | References |
|---|---|---|
| *Serpula himantioides* | | |
| Whewellite<br>Weddellite | Boar and walrus tusks | [15] |
| Calcium oxalates | High-purity gypsum ($CaSO_4$), and gypsum amended with 1% $FeSO_4$. | [16] |
| Calcium oxalates | Pure gypsum | [17] |
| Weddellite | Gypsum blocks | [18] |
| Weddellite<br>Whewellite | The natural dihydrate form of calcium sulfate, $CaSO_4 \cdot 2H_2O$ (gypsum) | [19] |
| Calcium oxalates | Zinc-containing ores (Zn sulfide) | [20] |
| Manganese oxalate trihydrate, Manganese oxalate dihydrate | Birnessite $[(Na_{0.3}Ca_{0.1}K_{0.1})(Mn^{4+},Mn^{3+})2O_4 \cdot 1.5H_2O]$. | [21] |
| Lead oxalate-like crystals | Lead sulfide (PbS) | [22] |
| *Serpula lacrymans* | | |
| Calcium oxalates | Lime mortar | [23] |
| Calcium oxalates | High-purity gypsum ($CaSO_4$), and gypsum amended with 1% $FeSO_4$. | [16] |
| Weddellite | Soil block with sphagnum and vermiculite with wood blocks of southern yellow pine | [3] |
| Calcium oxalates | Blocks of three types of Scottish building sandstone | [24] |
| *Coniophora puteana* | | |
| Weddellite | Soil block with sphagnum and vermiculite with wood blocks of the southern yellow pine soil block | [3] |
| Weddellite | Wood blocks of Pinus sylvestris (Scots pine) and Fagus sylvatica (European beech) | [25] |
| *Antrodia xantha* | | |
| Moolooite | Wood blocks of Japanese cedar treated with copper sulfate ($CuSO_4$) | [6] |

The goal of the present work is to clarify the contribution of brown rot fungi to oxalate formation in nature and the prospects for their use in modern environmentally friendly biotechnologies.

The specific objectives of the study are as follows:

(1) to find oxalates formed under the action of brown rot fungi on stone in natural conditions and propose a model for their formation;
(2) to synthesize analogs of biofilm oxalate minerals and oxalates of toxic heavy metals on different mineral substrates under the action of various brown rot fungi;
(3) to compare brown rot fungi species differing in biochemical activity and underlying mineral substrates differing in density and chemical composition and their effect on oxalate formation in experimental conditions;
(4) to compare the features of oxalate formation under the action of brown rot fungi and soil fungi widely used in model experiments and recommended for application in environmental biotechnologies [26–33].

## 2. Materials and Methods

### *2.1. Sampling*

The search for brown rot fungi in the zone of contact between wood and rock was carried out in the adit of the Rookgoselga mine (Tulomozerskaya group of Fe-deposits, Pryazhinsky district, South Karelia), abandoned in the 1930s (Figure 1a). High humidity and even partial flooding, and the presence of old wooden structures in the mine create favorable conditions for the development of brown rot fungi. These fungi were identified on the bases of branched cords of mycelium (Figure 1b). Samples of old wooden logs and adjacent carbonate rock with mycelium of brown rot fungi were collected into sterile containers.

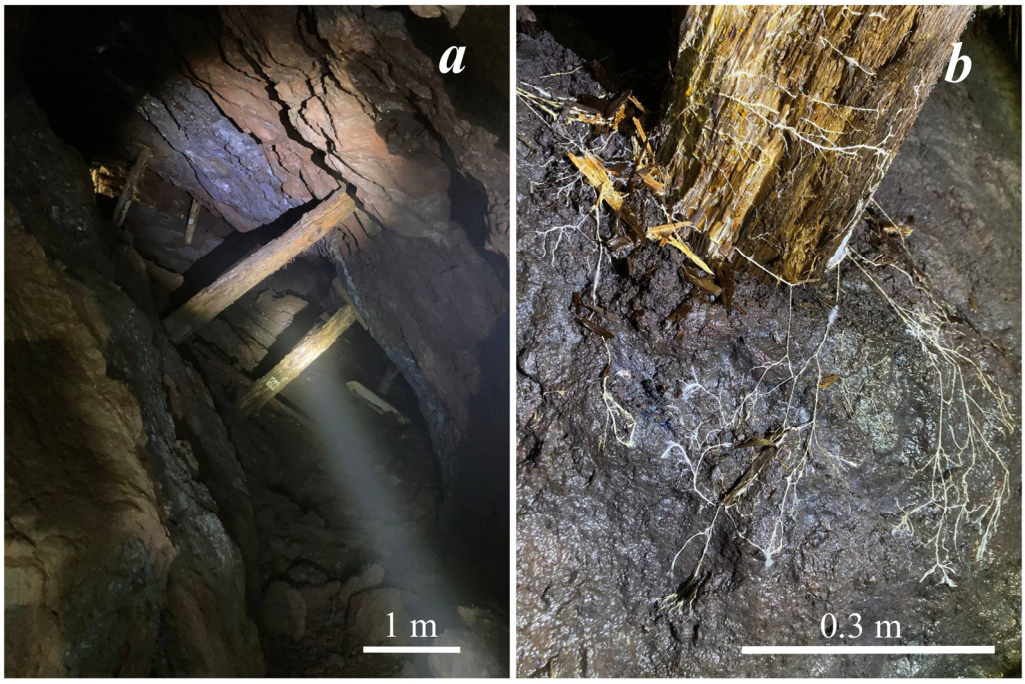


**Figure 1.** Sampling sites: (**a**) general view of the abandoned Rogoselga adit, (**b**) brown rot fungi cords on a damaged wood and carbonate rock.

### *2.2. Model Experiments*

Oxalate-forming brown rot fungi (Table 1) were selected for experiments: *Serpula himantioides*, *Serpula lacrymans*, *Antrodia xantha*, and *Coniophora puteana*. These species differ in their ability to produce organic acids including oxalic acid as well as their cellulose decomposition activity [14]. Fungal strains for the experiments (Table 2) were

obtained from the Komarov Botanical Institute Basidiomycetes Culture Collection (LE-BIN, WDCM1015). All strains were stored in the collection in cryovials at −80 °C with 10% glycerol as a cryoprotectant. The strains were cultivated on a glucose-peptone agar nutrient medium—GPA (glucose—10, peptone—3, $MgSO_4$—0.5, $CaCl_2$—0.05, $ZnSO_47H_2O$—0.01, $FeSO_4$ $7H_2O$—0.005, $KH_2PO_4$—0.6, $K_2HPO_4$—0.4, agar—20 g/L). Fungi showed active growth in this medium.

**Table 2.** Characterization of brown rot fungi strains from Komarov Botanical Institute Basidiomycetes Culture Collection (LE-BIN, WDCM1015).

| Strain Number in the LE-BIN Collection | Fungus Name | Origin | Collection Year | Strain Number in the NCBI Genbank |
|---|---|---|---|---|
| 1029 | *Antrodia xantha* (Fr.) Ryvarden. | Russia | 1996 | KY433983 |
| 1370 | *Coniophora puteana* (Schumach.) P. Karst. | Cuba | 1984 | KY433978 |
| 1368 | *Serpula himantioides* (Fr.) P. Karst. | Germany | 1997 | KY352492 |
| 1192 | *Serpula lacrymans* (Wulfen) J. Schröt. | Russia | 2000 | KY352493 |

A wide range of underlying mineral substrates differing in density and chemical composition (see Table 3 in section Results) were used. We selected the compositions of mineral substrates to obtain analogs of biofilm oxalate minerals and oxalates of toxic heavy metals. All selected mineral substrates in model experiments with the participation of chosen four species of brown rot fungi were previously not used. Samples of minerals and rocks were collected by us in expeditions and obtained from the collections of mineralogical museums, research institutes, and individuals (Table 3). To compare the features of oxalate formation under the action of brown rot and soil fungi, we chose the fungus *Aspergillus niger*, which is an active producer of oxalic acid and widely used in model experiments and often used in biotechnologies [33–40].

**Table 3.** Characterization of the underlying stone substrates used in model experiments.

| Mineral Composition | Main Mineral | Formula | Density, g/cm$^3$ [41] | Origin |
|---|---|---|---|---|
| Fine-grained homogeneous calcite marble with rare inclusions of small pyrite crystals | Mg-bearing calcite MgO content does not exceed 1.08 wt% | $(Ca, Mg)_1$ $(CO_3)$ | 2.71 | The restoration company "Heritage", Saint Petersburg, Russia |
| Fluorapatite crystal | Cl-bearing fluorapatite (Cl~1.17 wt%) | $Ca_5(PO_4)_3(F, Cl)$ | 3.1–3.25 | Slyudyanka mineral deposit, Irkutsk region, Russia |
| Magnesite contains a small amount of small grains of dolomite and quartz. Chlorite aggregate with apatite was found in interstices | Magnesite FeO (up to 4.94 wt%), CaO (up to 0.67 wt%) | $(Mg, Fe, Ca)_1(CO_3)$ | 2.98–3.02 | Satka deposit, Ural, Russia |
| Cerussite | Cerussite | $Pb(CO_3)$ | 6.53–6.57 | Central Scientific and Research Geological Museum of Academician F.N. Chernyshev (TSNIGR Museum), Saint Petersburg, Russia |

**Table 3.** *Cont.*

| Mineral Composition | Main Mineral | Formula | Density, g/cm$^3$ [41] | Origin |
|---|---|---|---|---|
| Hollandite in the form of entangled fibrous, reniform aggregates | Hollandite Sometimes there is an admixture of Fe (no more than 1.35 wt% FeO) | $Ba(Mn^{2+},Mn^{4+})_8O_{16}$ | 4.95 | U. M. Bronzova collection |
| Siderite, impurity phases are pyrite, muscovite, quartz and montmorillonite | Siderite | $(Fe_{0.85}, Mg_{0.1}, Mn_{0.05})_1CO_3$ | 3.96 | Dalnegorsk field, Primorsky Territory, Far East, Russia |
| Pyrrhotite, in rock ore largely replaced by poorly crystallized iron oxides and hydroxides. Quartz, kaolinite, albite are present as impurity phases. Biotite was found in some areas | Pyrrhotite | $Fe_{1-x}S_1$ | 4.58–4.65 | Pyrrhotite Gorge deposit, Khibiny mountains, Kola Peninsula, Russia |
| Malachite synthetic homogeneous | Malachite Fe may be present (up to 3.06 wt%) | $Cu_2(CO_3)(OH)_2$ | 3.6–4.05 | Synthesized (patent pending RU2159214) |

The experiments were carried out in liquid glucose-peptone (GPL) medium at room temperature with pH control of the cultural liquid (initial pH value 5.5). Mineral blocks (~1 × 0.5 × 0.5 cm) were put on the bottom of plastic Petri dishes and 20 mL of liquid medium was added. Inoculation was carried out by mycelium fragments of selected fungal strains from a 10-day-old fungal culture obtained on glucose-peptone agar (GPA) medium. The duration of the experiments was 30 days (on marble, 8 and 19 days). All syntheses were made in triplicate. The control experiments were carried out without fungi.

### *2.3. Methods*

Stone substrates, the mycelium of brown rot fungi, and products of biomineralization were investigated by X-ray, microscopy, and spectroscopy methods.

#### 2.3.1. Optical Microscopy

The development of the fungi during the experiment was observed using Leica optical stereomicroscope.

#### 2.3.2. Powder X-ray Diffraction (PXRD)

The determination of the phase composition of the stone substrates and products of biomineralization was carried out by the PXRD method. Equipment and methods were described in detail in our previous works [35–40].

#### 2.3.3. Scanning Electron Microscopy (SEM) and Energy-Dispersive Microanalysis (EDX)

Morphological studies of the formed crystals and their intergrowths and the elemental composition of stone substrates and crystalline products were carried out using SEM and EDX EMPA (electron microprobe analyzer). Equipment and methods were described in detail in our previous works [35–40]. The quantitative elemental composition of the stone substrates was determined on epoxy-mounted, polished, and carbon-coated samples mounted on the base of a Pegasus 4000 (EDAX, USA) analytical fitting, using the following standards: pure iron (Fe), pure manganese (Mn), pure copper (Cu), Calcite ($CaCO_3$), Dolomite ($MgCa(CO_3)_2$), Apatite ($Ca_5(PO_4)_3F$), Barite ($BaSO_4$), and lead (II) telluride (PbTe). EDX spectra were obtained under 20 kV accelerating voltage and 8.6nA beam current.

## 3. Results

### *3.1. Findings of Calcium Oxalates in the Rogoselga Adit*

Old wooden logs in the abandoned Rogoselga adit showed signs of destruction by brown rot fungi (Figure 1). On the surface of the timber, the cords of brown rot fungi mycelium were clearly visible. They extended also on the surface of adjacent carbonate rock (calcite, dolomite) with hematite streaks. Using PXRD and SEM with EDX spectroscopy, the presence of calcium oxalates (whewellite and weddellite) was shown (Figure 2). Oxalate crystals are along the fungal hyphae on both rock and wood (Figure 2b–d).Whewellite prevails and presents as lamellar crystals less than 5 μm in size. Weddellite crystals are dipyramidal or dipyramidal-prismatic. The prism face is poorly developed. The predominant weddellite crystals are 5–10 μm in size and the largest crystals reach 25–30 μm (Figure 2d). Traces of crystals dissolution and splitting are often visible.

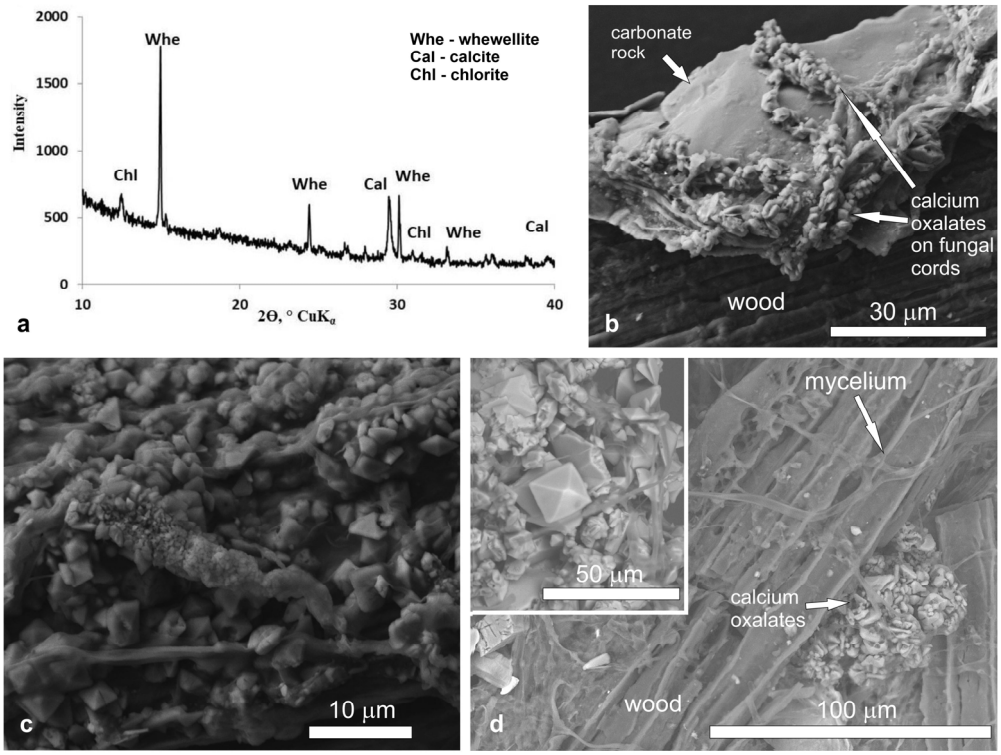


**Figure 2.** X-ray diffraction pattern (**a**) and SEM images (**b**–**d**) of calcium oxalates in the Rogoselga adit: (**b**)—underlying substrate (old timber and adjoining carbonate rock) with brown rot fungi and calcium oxalates on fungal cords; (**c**) numerous small crystals of whewellite and weddellite on fungal cords localized mainly on carbonate rock; (**d**)—large dipyramidal crystals of weddellite (incut) among numerous small crystals of whewellite on old timber.

### *3.2. Oxalate Formation in Model Experiment*

#### 3.2.1. Characterization of Underlying Stone Substrates

The results of the study using PXRD and EDX spectroscopy showed that the mineral substrates selected for the model experiment are represented by carbonates of various metals as well as hollandite, fluorapatite, and pyrrhotite (Table 3). Their density varies markedly from 2.71 (calcite marble) to 6.57 (lead carbonate).

#### 3.2.2. Crystallization on Different Rock and Minerals

*On marble.* On the surface of the marble, calcium oxalate crystals of weddellite and whewellite were formed under the action of four fungi: *Serpula himantioides*, *Serpula lacrymans*, *Coniophora puteana*, and *Antrodia xantha* (Tables 4 and 5, Figures 3 and 4). The formation of calcium oxalates occurred under the action of *Serpula himantioides* and

*Antrodia xantha* on the 8th day of the experiment at pH values of 3.5 and 4.5, respectively (Table 5) and under the action *of Serpula lacrymans* and *Coniophora puteana* on the 19th day at pH values from 3 and 2.5, respectively. There is a strong acidification of the medium by 19 and 30 days of the experiment. The number of crystals increases, but their phase composition does not change on the 30th day of the experiment. The formation of calcium oxalates monohydrate whewellite and dehydrated weddellite occurred under the action of *Serpula himantioides* and *Serpula lacrymans*. There were many more weddellite crystals than whewellite. Weddellite crystals were dipyramidal or dipyramidal-prismatic, and the prism face is either almost undeveloped or poorly developed (Figure 4a). Their size varies from 20 μm to 70 μm. Calcium oxalate monohydrate whewellite appears as lamellar crystals and their intergrowths reaching up to 75 μm in size (under the action of *Serpula lacrymans*, Figure 5a). Under the influence of *Coniophora puteana*, the formation of whewellite occurred in a much larger amount, and weddellite crystals were single crystals. Under the action of *Antrodia xantha*, only crystals of calcium oxalates monohydrate whewellite were formed (Figure 5b). The size of the whewellite crystals intergrowths varied from 25μm to 100 μm. The weddellite and whewellite crystals formed under the action of all studied fungi completely covered the marble surface, forming a continuous layer (Figures 4a and 5a,b). The formation of calcium oxalates on marble under the action of fungi occurred at pH values from 2 to 4.5 (Table 5).

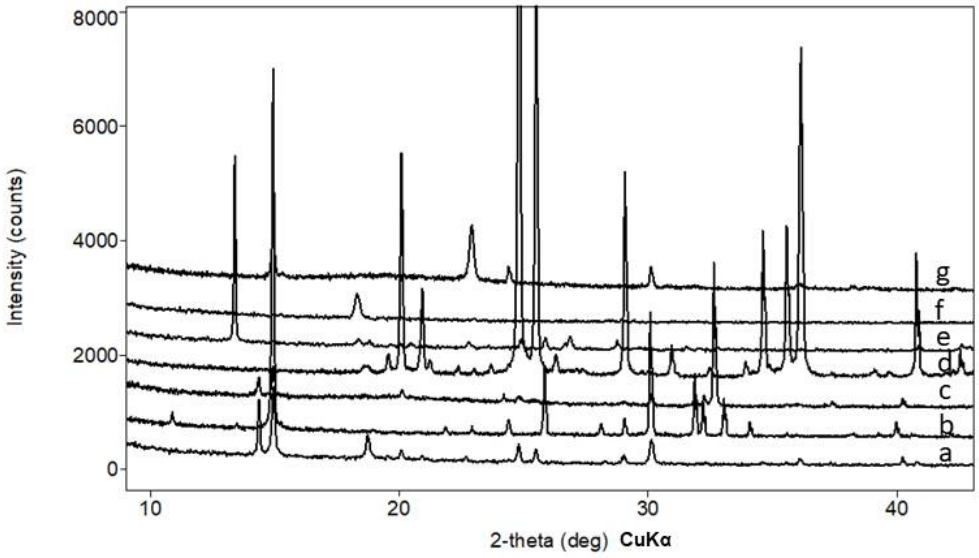


**Figure 3.** Selected X-ray diffraction pattern of the oxalates crystals (underlying stone substrate's reflections are also present): a—weddellite and whewellite formed under the action of *Serpula himantioides* on marble; b—whewellite, *Serpula himantioides*, fluorapatite; c—glushinskite and whewellite, *Serpula himantioides*, magnesite; d—anhydrous lead oxalate, *Coniophora puteana*, cerussite; e—falottaite and lindberghite, *Coniophora puteana*, hollandite; f—humboldtine, *Antrodia xantha*, siderite; g—moolooite, *Antrodia xantha*, synthetic malachite.

**Table 4.** The crystalline products of the reaction between mineral substrates with four species of brown rot fungi vs. pH of crystallization medium (SEM and PXRD).

| Species of Brown Rot Fungi | | Underlying Mineral Substrate | | | | | | | |
|---|---|---|---|---|---|---|---|---|---|
| | | **Marble** | **Fluorapatite** | **Magnesite** | **Cerussite** | **Hollandite** | **Siderite** | **Pyrrhotite** | **Malachite** |
| *Serpula himantioides* | pH | 2.5 | 2 | 2.5 | 2 | 3 | 3 | 2.5 | 3 |
| | SEM with EDXS | weddellite, whewellite | whewellite | glushinskite *, weddellite, whewellite | anhydrous lead oxalate, whewellite | falottaite, lindbergite | humboldtine * | humboldtine * | moolooite * |
| | PXRD | weddellite, whewellite | whewellite | glushinskite *, weddellite, whewellite | anhydrous lead oxalate | falottaite, lindbergite | humboldtine * | humboldtine * | moolooite * |
| *Serpula lacrymans* | pH | 3 | 5.5 | 5 | 3 | - | - | - | - |
| | SEM with EDXS | weddellite, whewellite | whewellite | - | anhydrous lead oxalate *, whewellite | - | - | - | - |
| | PXRD | weddellite, whewellite | - | - | whewellite | - | - | - | - |
| *Coniophora puteana* | pH | 3 | 3 | 3.5 | 2.5 | 5 | 5.5 | 2 | 3.5 |
| | SEM with EDXS | weddellite, whewellite | whewellite | whewellite | whewellite anhydrous lead oxalate * | falottaite *, lindbergite * | humboldtine * | humboldtine * | moolooite * |
| | PXRD | weddellite, whewellite | whewellite | whewellite | anhydrous lead oxalate * | falottaite * | - | humboldtine * weddellite, whewellite | moolooite * |
| *Antrodia xantha* | pH | 2 | 3.5 | 4 | 3.5 | 2 | 2 | 4 | 2.5 |
| | SEM with EDXS | whewellite * | whewellite * | whewellite *, weddellite * | anhydrous lead oxalate *, whewellite *, weddellite * | whewellite * lindbergite * | humboldtine * | whewellite * | moolooite |
| | PXRD | whewellite * | whewellite * | whewellite *, weddellite * | anhydrous lead oxalate *, whewellite *, weddellite * | whewellite * lindbergite * | humboldtine * | whewellite * | moolooite |

*—oxalates were obtained on specific mineral substrates under the action of one of the four species of brown rot fungi for the first time.

**Table 5.** The crystalline products of the reaction between marble and four species of brown rot fungi vs. pH of crystallization medium (SEM and PXRD).

| Species of Brown Rot Fungi | | Days | |
|---|---|---|---|
| | | **8** | **19** |
| *Serpula himantioides* | pH | 3.5 | 2.5 |
| | SEM with EDXS, PXRD | weddellite | weddellite whewellite |
| *Serpula lacrymans* | pH | 4.5 | 3 |
| | SEM with EDXS, PXRD | - | weddellite whewellite |
| *Coniophora puteana* | pH | 5 | 2.5 |
| | SEM with EDXS, PXRD | - | weddellite whewellite |
| *Antrodia xantha* | pH | 4.5 | 2 |
| | SEM with EDXS, PXRD | whewellite | whewellite |

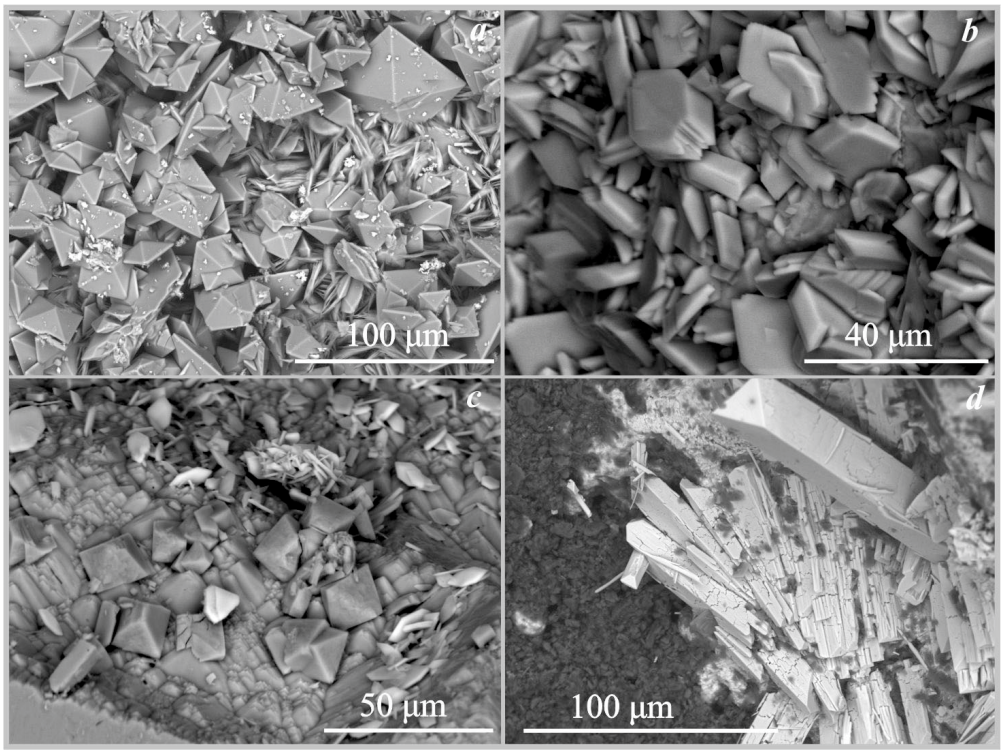


**Figure 4.** SEM images of the oxalate crystals formed under the action of *Serpula himantioides*: (**a**)—weddellite and whewellite on marble; (**b**)—whewellite on fluorapatite; (**c**)—glushinskite and whewellite on magnesite; (**d**)—anhydrous lead oxalate on cerussite.

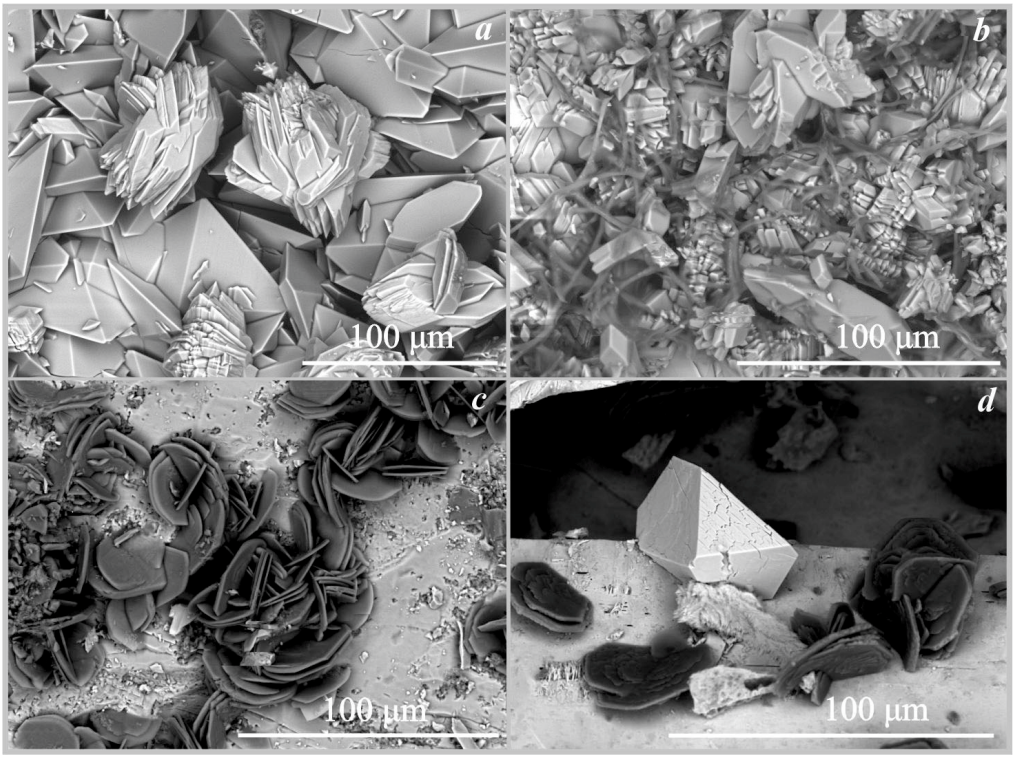


**Figure 5.** SEM images of the oxalate crystals formed under the action of *Serpula lacrymans*: (**a**)—weddellite and whewellite on marble; (**b**)—whewellite on marble (under the action of *Antrodia xantha*); (**c**)—whewellite on fluorapatite; (**d**)—anhydrous lead oxalate and whewellite on cerussite.

*On fluorapatite.* The formation of calcium oxalates monohydrate whewellite under the action of the four fungi on the surface of fluorapatite occurred at pH values from 2 to 5.5 (Table 4, Figure 3). Whewellite was represented by lamellar pseudo-hexagonal crystals with straight or curved edges and their intergrowths (Figure 4b). The size of the whewellite crystals and their intergrowths varies from 20 µm to 50 µm. Intensive splitting of the crystals and the formation of dovetail-type twins were observed. Whewellite crystals covered the surface of the fluorapatite in a completely continuous layer. Under the action of the fungus *Serpula lacrymans*, the formation of calcium oxalate whewellite occurred in a small amount and the crystals were identified only by SEM and EMPA data (Figure 5c) and formed intergrowths of rose-like aggregates 25–30 µm in size.

*On magnesite.* The formation of magnesium oxalate glushinskite on the surface of magnesite was recorded only under the action of the fungus *Serpula himantioides* (Table 4, Figures 3 and 4c) at pH = 2.5. According to SEM and EMPA data, glushinskite was represented by individual short-prismatic almost isometric monoclinic crystals 15–25 µm in size (Figure 4c). In addition to magnesium oxalate, the formation of calcium oxalates weddellite and whewellite was also recorded on the surface of magnesite under the action of *Serpula himantioides*, *Coniophora puteana*, and *Antrodia xantha* at pH = 2.5 and pH = 4 (Table 4).

*On cerussite.* The formation of anhydrous lead oxalate was recorded on the surface of cerussite (Figures 3, 4d and 5d, Table 4) under the action of the four species of brown rot fungi at pH = 2 and pH = 3.5. It should be noted that under the action of the fungus *Serpula lacrymans*, the formation of lead oxalate occurred, but only in small amounts. Only single crystals of anhydrous lead oxalate were recorded on the surface of cerussite by SEM and EMPA data (Figure 5d, Table 4). Lead oxalate was represented by individual triclinic well-faceted crystals 30–40 µm in size. In addition to lead oxalate, calcium oxalates also appeared on the surface of cerussite: under the influence of *Serpula himantioides* and *Serpula lacrymans*—whewellite, and, under the influence of

*Coniophora puteana*, *Antrodia xantha*—whewellite and weddellite (Table 4). According to SEM and EMPA data, the lead oxalate formed under the action of *Coniophora puteana*, *Antrodia xantha*, and *Serpula himantioides* was represented by numerous spindle-shaped intergrowths of elongated multi-headed skeletal crystals 100–200 µm in size (Figure 4d).

*On hollandite.* The formation of manganese oxalates was recorded on the surface of hollandite under the action of three fungi: trihydrate falottaite and dehydrate lindbergite under the influence of *Serpula himantioides* and *Coniophora puteana*, and lindbergite under the influence of *Antrodia xantha* (Figures 3, 6a and 7a, Table 4). The formation of oxalates occurred at pH values from 2 to 5. According to SEM and EMPA data, the falottaite was represented by very large flat needle-like crystals (Figures 6a and 7a) 200 µm–1 mm in size, and lindbergite was obtained as spherulite-like intergrowths of plate-like crystals 70–400 µm in size. In addition to manganese oxalates, the formation of calcium oxalate whewellite was also recorded on the surface of hollandite under the action of *Antrodia xantha* at pH = 2 (Table 4).

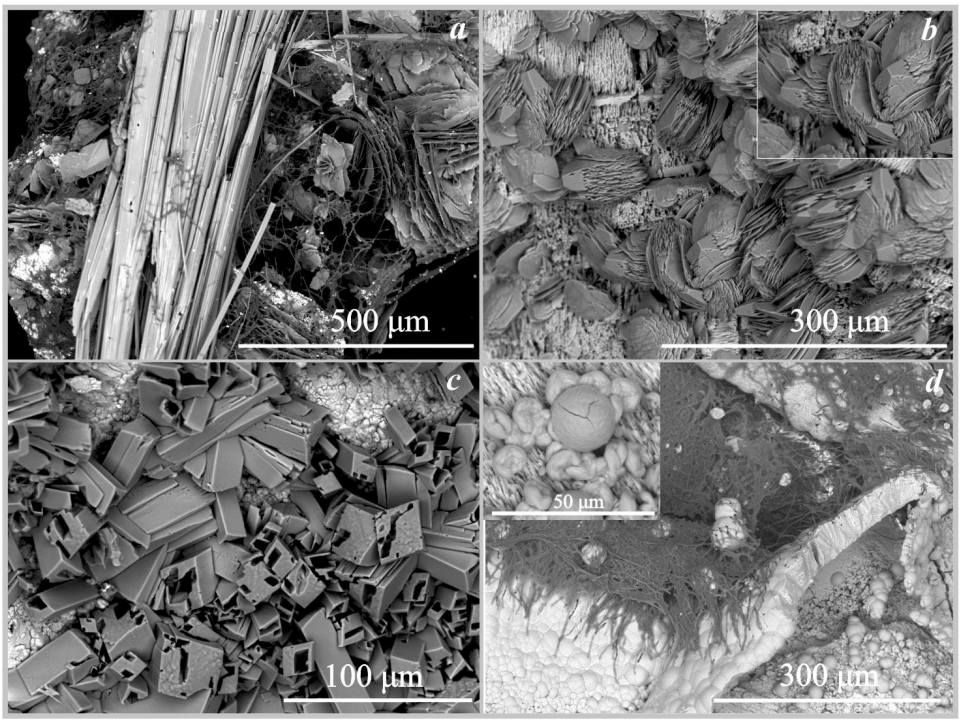


**Figure 6.** SEM images of the oxalate crystals formed under the action of *Serpula himantioides*: (**a**)—falottaite and lindbergite on hollandite; (**b**)—humboldtine on siderite; (**c**)—humboldtine on pyrrhotite; (**d**)—moolooite on synthetic malachite.

*On siderite.* The formation of iron oxalate humboldtine was recorded on the surface of siderite under the action of three fungi *Coniophora puteana, Serpula himantioides, and Antrodia xantha* at pH values from 2 to 5.5 (Table 4, Figures 6b and 7b). According to SEM and EMPA data, the humboldtine was represented by elongated monoclinic crystals of prismatic habit and their intergrowths 80–100 µm in size. Under the action of the fungus *Serpula himantioides*, a strong splitting of individual large humboldtine crystals was observed (Figure 6b). According to EDX data, humboldtine contained small amounts of manganese and magnesium.

*On pyrrhotite.* The formation of iron oxalate humboldtine was recorded on the surface of pyrrhotite under the action of two fungi *Coniophora puteana* and *Serpula himantioides* at pH values from 2 to 2.5 (Table 4, Figure 6c). The crystals of humboldtine have traces of dissolution. According to EDX data, iron oxalate contained small amounts of magnesium.

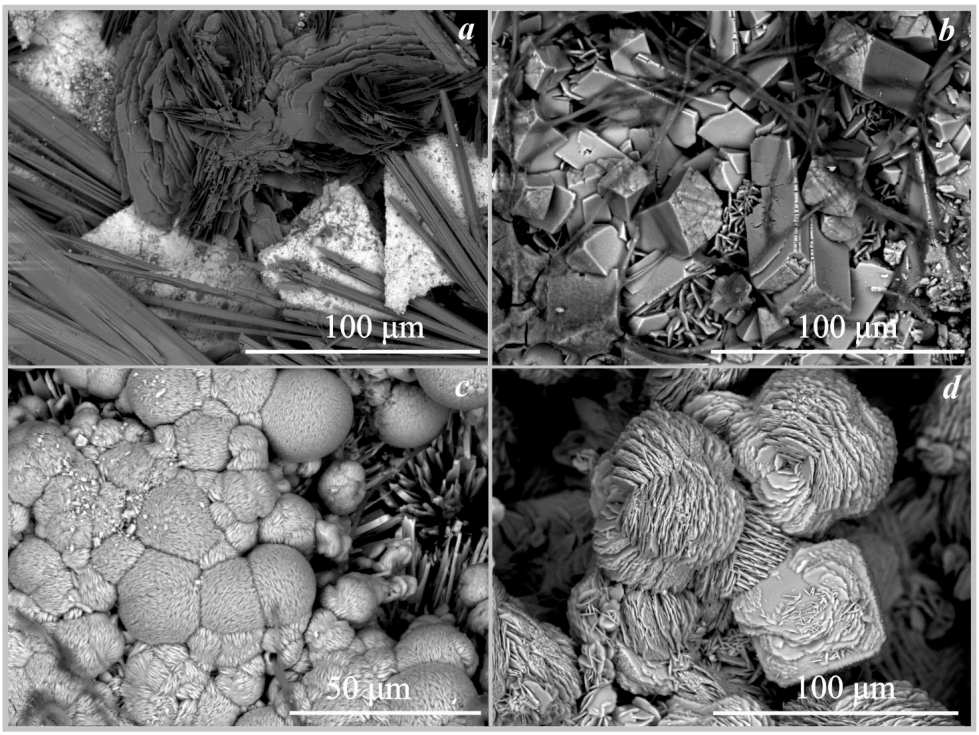


**Figure 7.** SEM images of the oxalate crystals (**a**)—falottaite and lindbergite on hollandite formed under the action of *Coniophora puteana*; (**b**)—humboldtine, whewellite on siderite formed under the action of *Antrodia xantha*; (**c**)—moolooite on synthetic malachite formed under the action of *Antrodia xantha*; (**d**)—moolooite on synthetic malachite formed under the action of *Coniophora puteana*.

*On synthetic malachite.* The formation of copper oxalate moolooite was recorded on the surface of synthetic malachite under the action of three fungi *Coniophora puteana*, *Serpula himantioides*, and *Antrodia xantha* at pH values from 2.5 to 3.5 (Table 4, Figures 6d and 7c,d). According to SEM and EMPA data, the moolooite was represented by "box-like" spherulite intergrowths, which are formed by perpendicular stacks of plate-like crystals 25–50 μm in size. Spherulite intergrowths of moolooite form a crust on the surface of malachite up to 70 μm thick (Figure 7d).

## 4. Discussion

### *4.1. Participation of Brown Rot Fungi in Oxalates Formation in Nature*

We found brown rot fungi and calcium oxalates crystals on carbonate rock in the Rogoselga adit (Figures 1 and 2). According to our observation, cords of brown rot fungi mycelium develop on stone substrates only in direct contact with damaged wooden logs. Oxalate crystals are seen not only on stone but also on wood substrates.

It can be assumed that brown rot fungi first settle on wood, accumulate biomass and begin to release enzymes and oxalic acid. This leads to the destruction of the wood. At some point after the accumulation of significant biomass, they start to move to the mineral substrate. Interaction of brown rot fungi with rocks and minerals initiates solubilization processes and in many cases leads to the creation of favorable conditions for oxalate crystallization. The humid environment in the Rogoselga adit significantly intensifies the ongoing destruction and crystallization processes. The elements washed out from rocks and minerals pass into the solution circulating in the closed space of the adit and fall on the surface of the wood. At this stage, the circulating solutions are saturated with oxalate ions, which creates favorable conditions for the formation of oxalates directly on the wood. The study of oxalates crystallization by brown rot fungi directly on wood in the absence of contact with mineral substrates is now in progress.

Our finding in the Rogoselga adit confirms the assumptions that the frequent occurrence of metal oxalates in subsurface space may be associated with the activity of brown rot fungi and other wood-rotting fungi inhabiting such conditions and producing oxalic acid.

The results of model experiments support the contention that brown rot fungi play a significant role in oxalate formation in natural conditions. We synthesized under the action of these fungi on the different minerals analogs of all known oxalate minerals found in biofilms (Tables 4 and 5): Ca-oxalates (whewellite, weddellite), Cu-oxalate moolooite, Mn-oxalate lindbergite, and Mg-oxalate glushinskite, and also iron oxalate humboldtine, the presence of which in biofilms is still questionable. Analogs of magnesium oxalate glushenskite and iron oxalate humboldtine under the action of brown rot fungi were synthesized for the first time. In addition, we synthesized Pb-oxalate, which together with zinc oxalate was previously found in lichen thalli [42], but has not yet been approved as a new mineral.

### *4.2. Prospects for the Use of Brown Rot Fungi in Modern Biotechnologies*

We synthesized under the action of brown rot fungi on the different minerals oxalates of the following toxic heavy metals: Pb, Cu, and Mn. Thus, brown rot fungi produce enough oxalic acid to convert cations in solution, including toxic ones, into insoluble oxalates. This indicates the prospects for the use of these fungi in biotechnology for bioremediation of the environment and enrichment of ores.

The contribution of the studied fungi to the formation of oxalates was different. The most active fungus *Serpula himantioides* formed oxalates in all variants of the experiments. At the same time, the least active in culture fungus *Serpula lacrymans*, known as one of the most common timber destructors, formed oxalates in only 3 out of 8 variants of the experiments. It should be noted that this fungus had a rather low growth rate in culture conditions, which probably affected its interaction with the mineral substrate. Under the influence of other fungi *Coniophora puteana* and *Antrodia xantha*, the formation of metal oxalates was less active than in the case of *Serpula himantioides*, but it was also obtained in all variants of the experiments.

Crystallization under the action of brown rot fungi occurred in a liquid medium under acidic conditions at pH 2.0–5.5 (Table 4). For comparison, under the action of the soil fungus *A.niger*, the pH values in the culture liquid on the surface of the different mineral substrates during oxalate formation occurred at a fairly close pH and varied from 2.5 to 5.0 [33,36,37,39,40].

As we have shown earlier, in the case of experiments with *A.niger*, the pH value depends not only on the intensity of the release of organic acids by fungi but also on the density of the underlying substrates [37–40]. Aggressive metabolic products of *A. niger* accumulate more easily on denser rock, which leads to a decrease in the pH at which oxalates crystallize. The pH values in experiments with brown rot fungi (Tables 4 and 5) are grouped only by fungal species. This indicates that in contrast to *A.niger* the contribution of the metabolic activity of brown rot fungi to crystallization medium acidification significantly exceeds the contribution of the underlying substrate. It is possible to rank the studied species by pH values: *Serpula himantioides* (pH = 2–3) > *Antrodia xantha* (pH = 2–4) > *Coniophora puteana* (pH = 2–5.5) > *Serpula lacrymans* (pH = 3–5.5). These results agree well with the contribution of these fungi in oxalate formation discussed above.

Thus, brown rot fungi (*Serpula himantioides, Antrodia xantha, Coniophora puteana*) form oxalates more intensively than soil fungus *A.niger*, which is associated with the active production of oxalic acid and biomass growth. This is also indicated by the data of Adeyemi [22], on a more intense lead accumulation in the mycelium of *Serpula himantioides* compared to the mycelium of *A.niger*. In addition, brown rot fungi do not spore in culture and are safer than *A.niger*. All of the above confirm the prospects of using wood-rotting fungi in modern environmentally friendly biotechnologies (shown by the example of brown rot fungi).

## 5. Conclusions

In the present work, we clarified the contribution of brown rot fungi to oxalate formation in nature and the prospects for their use in modern environmentally friendly biotechnologies.

We first found oxalates formed under the action of brown rot fungi on stone in natural conditions (Rogoselga adit, Karelia, Russia), proposed a model for their formation, and thus confirmed the hypothesis that frequent occurrence of metal oxalates in subsurface space (mines, adits, and so on) may be associated with the activity of these fungi.

We synthesized under the action of brown rot fungi (*Serpula himantioides*, *Serpula lacrymans*, *Coniophora puteana*, and *Antrodia xantha*) analogs of biofilm oxalate minerals and oxalates of toxic heavy metals (Pb, Cu, Mn) on different mineral substrates and showed that in contrast to *A. niger* the contribution of the metabolic activity of brown rot fungi to crystallization medium acidification significantly exceeds the contribution of the underlying substrate.

Clearly, the contribution of wood-rotting fungi in biomineralization in nature is quite significant and is not inferior to the contribution of microscopic fungi and other microorganisms. The application of brown rot fungi such as *Serpula himantioides*, *Coniophora puteana* and *Antrodia xantha* in modern biotechnologies appears to be very promising but requires further research.

**Author Contributions:** Conceptualization, D.Y.V., M.S.Z., A.R.I. and O.V.F.-K.; Methodology, M.S.Z., A.R.I. and S.Y.J.; Investigation, M.S.Z., A.R.I. and S.Y.J.; Writing—Original Draft Preparation, D.Y.V., M.S.Z., A.R.I. and S.Y.J.; Writing—Review & Editing, D.Y.V., M.S.Z., A.R.I., S.Y.J. and O.V.F.-K.; Visualization, M.S.Z., A.R.I. and S.Y.J. All authors have read and agreed to the published version of the manuscript.

**Funding:** This research was funded by the Russian Science Foundation (grant 19-17-00141).

**Data Availability Statement:** Not applicable.

**Acknowledgments:** The laboratory research was carried out in the Research Park of Saint Petersburg State University, the SEM investigations—in the "Resource Center Microscopy and Microanalysis (RCMM)" and in the Centre for Geo-Environmental Research and Modelling (Geomodel), the XRD measurements—in the X-Ray Diffraction Centre. We are grateful to the reviewers for their useful comments. Samples of pyrrhotite and siderite were prepared in the Sample Preparation Laboratory of the Institute of Earth Sciences, St. Petersburg State University. The authors would like to thank I.V. Borisov for organizing the expedition to the Rogoselga adit (South Karelia).

**Conflicts of Interest:** The authors declare no conflict of interest.

## References

1. Dutton, M.V.; Evans, C.S.; Atkey, P.T.; Wood, D.A. Oxalate production by Basidiomycetes, including the white-rot species *Coriolus versicolor* and *Phanerochaete chrysosporium*. *Appl. Microbiol. Biotechnol.* **1993**, *39*, 5–10. [CrossRef]
2. Dutton, M.V.; Evans, C.S. Oxalate production by fungi: Its role in pathogenicity and ecology in the soil environment. *Can. J. Microbiol.* **1996**, *42*, 881–895. [CrossRef]
3. Hastrup, A.C.S.; Green, F., III; Lebowb, P.K.; Jensen, B. Enzymatic oxalic acid regulation correlated with wood degradation in fourbrown-rot fungi. *Int. Biodeterior. Biodegrad.* **2012**, *75*, 109–114. [CrossRef]
4. Chen, L.; Zhang, X.; Zhang, M.; Zhu, Y.; Zhuo, R. Removal of heavy-metal pollutants by white rot fungi: Mechanisms, achievements, and perspectives. *J. Clean. Prod.* **2022**, *35*, 413–681. [CrossRef]
5. Kaewdoung, B.; Sutjaritvorakul, T.; Gadd, G.M.; Whalley, A.J.S.; Sihanonth, P. Heavy Metal Tolerance and Biotransformation of Toxic Metal Compounds by New Isolates of Wood-Rotting Fungi from Thailan. *Geomicrobiol. J.* **2016**, *33*, 283–288. [CrossRef]
6. Hattori, T.; Hisamori, H.; Suzuki, S.; Umezawa, T.; Yoshimura, T.; Sakai, H. Rapid copper transfer and precipitation by wood-rotting fungi can effect copper removal from copper sulfate-treated wood blocks during solid-state fungal treatment. *Int. Biodeterior. Biodegrad.* **2015**, *97*, 195–201. [CrossRef]
7. Demartin, F.; Campostrini, I.; Ferretti, P.; Rocchetti, I. Fiemmeite $Cu_2(C_2O_4)(OH)_2$ $2H_2O$, a New Mineral from Val di Fiemme, Trentino, Italy. *Minerals* **2018**, *8*, 248. [CrossRef]
8. Atencio, D.; Coutinho, J.M.V.; Graeser, S.; Matioli, P.A.; Menezes Filho, L.A.D. Lindbergite, a new manganese oxalate dihydrate from Boca Rica mine, Galiléia, Minas Gerais, Brazil, and Parsettens, Oberhalbstein, Switzerland. *Am. Mineral.* **2004**, *89*, 1087–1091. [CrossRef]

9. Rieck, B.; Giester, G.; Lengauer, C.; Nasdala, L. Katsarosite, IMA 2020-014—CNMNC Newsletter 57. *Eur. J. Mineral.* **2020**, *32*, 495–499.
10. Guggiari, M.; Bloque, R.; Aragno, M.; Verrecchia, E.; Job, D.; Junier, P. Experimental calcium-oxalate crystal production and dissolution by selected wood-rot fungi. *Int. Biodeterior. Biodegrad.* **2011**, *65*, 803–809. [CrossRef]
11. Jarosz-Wilkolazka, A.; Gadd, G.M. Oxalate production by wood-rotting fungi growing in toxic metal-amended medium. *Chemosphere* **2003**, *52*, 541–547. [CrossRef] [PubMed]
12. Schmidt, O. Indoor wood-decay basidiomycetes: Damage, causal fungi, physiology, identification and characterization, prevention and control. *Mycol. Progress.* **2007**, *6*, 261–279. [CrossRef]
13. Watkinson, S.C.; Eastwood, D.C. Serpula lacrymans, Wood and Buildings. *Adv. Appl. Microbiol.* **2012**, *78*, 121–149. [PubMed]
14. Kolker, T.L.; Psurtseva, N.V.; Sazanova, K.V.; Vlasov, D.Y. Characteristics of domestic fungi maintaining in the Komarov Botanical Institute Basidiomycetes Culture Collection. *Mycol. Fytopatologia* **2018**, *52*, 398–407.
15. Pinzari, F.; Tate, J.; Bicchieri, M.; Rhee, Y.J.; Gadd, G.M. Biodegradation of ivory (natural apatite): Possible involvement of fungal activity in biodeterioration of Lewis Chessman. *Environ. Microbiol.* **2013**, *15*, 1050–1062. [CrossRef]
16. Schilling, J.S. Effects of calcium-based materials and iron impurities on wood degradation by the brown rot fungus *Serpula lacrymans*. *Holzforsch.* **2010**, *64*, 93–99. [CrossRef]
17. Schilling, J.S.; Bissonnette, K.M. Iron and calcium translocation from pure gypsum and iron-amended gypsum by two brown rot fungi and a white rot fungus. *Holzforschung* **2008**, *62*, 752–758. [CrossRef]
18. Schilling, J.S.; Jellison, J. Extraction and translocation of calcium from gypsum during wood biodegradation by oxalate-producing fungi. *Int. Biodeterior. Biodegrad.* **2007**, *60*, 8–15. [CrossRef]
19. Gharieb, M.; Sayer, J.A.; Gadd, M.G. Solubilization of natural gypsum ($CaSO_4$ $2H_2O$) and the formation of calcium oxalate by *Aspergillus niger* and *Serpula himantioides*. *Mycol. Res.* **1998**, *102*, 825–830. [CrossRef]
20. Wei, Z.; Liang, X.; Pendlowski, H.; Hillier, S.; Suntornvongsagul, K.; Sihanonth, P.; Gadd, M.G. Fungal biotransformation of zinc silicate and sulfide mineral ores. *Environ. Microbiol.* **2013**, *15*, 2173–2186. [CrossRef]
21. Wei, Z.; Hillier, S.; Gadd, M.G. Biotransformation of manganese oxides by fungi: Solubilization and production of manganese oxalate biominerals. *Environ. Microbiol.* **2012**, *14*, 1744–1752. [CrossRef] [PubMed]
22. Adeyemi, A.O. Biological immobilization of lead from lead sulphide by *Aspergillus niger* and *Serpula himantioides*. *Int. J. Environ. Res.* **2009**, *3*, 477–482.
23. Žofková, D.C.; Frankl, J.; Frankeova, D. Use of thermal analysis for the detection of calcium oxalate in selected forms of plastering exposed to the effects of *Serpula lacrymans*. *Acta Polytech.* **2021**, *61*, 511–515. [CrossRef]
24. Low, M.E.; Young, P.; Martin, J.; Palfreyman, W. Assessing the relationship between the dry rot fungus *Serpula lacrymans* and selected forms of masonry. *Int. Biodeterior. Biodegrad.* **2000**, *46*, 141–150. [CrossRef]
25. Ali, R.; Murphy, R.J.; Dickinson, D.J. Investigation of the extracellular mucilaginous materials produced by some wood decay fungi. *Mycol. Res.* **1999**, *103*, 1453–1461. [CrossRef]
26. Sayer, J.A.; Kierans, M.; Gadd, J.M. Solubilisation of some naturally occurring metal-bearing minerals, limescale and lead phosphate by *Aspergillus niger*. *FEMS Microbiol. Lett.* **1997**, *154*, 29–35. [CrossRef]
27. Sayer, J.A.; Cotter-Howells, J.D.; Watson, C.; Hillier, S.; Gadd, G.M. Lead mineral transformation by fungi. *Curr. Biol.* **1999**, *9*, 691–694. [CrossRef]
28. Fomina, M.; Hillier, S.; Charnock, J.M.; Melville, K.; Alexander, I.J.; Gadd, G.M. Role of oxalic acid overexcretion in transformations of toxic metal minerals by *Beauveria caledonica*. *Appl. Environ. Microbiol.* **2005**, *71*, 371–381. [CrossRef]
29. Sutjaritvorakul, T.; Gadd, M.G.; Suntornvongsagul, K.; Whalley, A.J.S.; Roengsumran, S.; Sihanonth, P. Sulubilization and transformation of insoluble zinc compounds by fungi isolated from a zinc mine. *Environ. Asia* **2013**, *6*, 42–46.
30. Gadd, G.M.; Bahri-Esfahani, J.; Li, Q.; Rhee, Y.J.; Wei, Z.; Fomina, M.; Liang, X. Oxalate production by fungi: Significance in geomycology, biodeterioration and bioremediation. *Fungal Biol. Rev.* **2014**, *28*, 36–55. [CrossRef]
31. Khan, I.; Aftab, M.; Shakir, S. Mycoremediation of heavy metal (Cd and Cr)–polluted soil through indigenous metallotolerant fungal isolates. *Environ. Monit. Assess.* **2019**, *191*, 585. [CrossRef] [PubMed]
32. Kang, X.; Csetenyi, L.; Gadd, G.M. Biotransformation of lanthanum by *Aspergillus niger*. *Appl. Microbiol. Biotechnol.* **2019**, *103*, 981–993. [CrossRef] [PubMed]
33. Vlasov, D.Y.; Frank-Kamenetskaya, O.V.; Zelenskaya, M.S.; Sazanova, K.V.; Rusakov, A.V.; Izatulina, A.R. The use of *Aspergillus niger* in modeling of modern mineral formation in lithobiotic systems. In *Aspergillus niger: Pathogenicity, Cultivation and Uses*; Nova Science Publishers: New York, NY, USA, 2020; pp. 1–123.
34. Sturm, E.V.; Frank-Kamenetskaya, O.V.; Vlasov, D.Y.; Zelenskaya, M.S.; Sazanova, K.V.; Rusakov, A.V.; Kniep, R. Crystallization of calcium oxalate hydrates by interaction of calcite marble with fungus *Aspergillus niger*. *Am. Mineral.* **2015**, *100*, 2559–2565. [CrossRef]
35. Rusakov, A.V.; Vlasov, A.D.; Zelenskaya, M.S.; Frank-Kamenetskaya, O.V.; Vlasov, D.Y. The crystallization of calcium oxalate hydrates formed by interaction between microorganisms and minerals. In *Biogenic—Abiogenic Interactions in Natural and Anthropogenic Systems*; Frank-Kamenetskaya, O.V., Panova, E.G., Vlasov, D.Y., Eds.; Springer: Cham, Switzerland, 2016; pp. 357–377.
36. Frank-Kamenetskaya, O.V.; Ivanyuk, G.Y.; Zelenskaya, M.S.; Izatulina, A.R.; Kalashnikov, A.O.; Vlasov, D.J.; Polyanskaya, E.I. Calcium Oxalates in Lichens on Surface of Apatite-Nepheline Ore (Kola Peninsula, Russia). *Minerals* **2019**, *9*, 656. [CrossRef]

37. Zelenskaya, M.S.; Rusakov, A.V.; Frank-Kamenetskaya, O.V.; Vlasov, D.Y.; Izatulina, A.R.; Kuz'mina, M.A. Crystallization of Calcium Oxalate Hydrates by Interaction of Apatites and Fossilized Tooth Tissue with Fungus *Aspergillus niger*. In *Processes and Phenomena on the Boundary Between Biogenic and Abiogenic Nature*; Lecture Notes in Earth System Sciences; Frank-Kamenetskaya, O., Vlasov, D., Panova, E., Lessovaia, S., Eds.; Springer: Cham, Switzerland, 2020; pp. 581–603.
38. Frank-Kamenetskaya, O.V.; Zelenskaya, M.S.; Izatulina, A.R.; Vereshchagin, O.S.; Vlasov, D.Y.; Himelbrant, D.E.; Pankin, D.V. Copper oxalate formation by lichens and fungi. *Sci. Rep.* **2021**, *11*, 24239. [CrossRef]
39. Zelenskaya, M.S.; Izatulina, A.R.; Frank-Kamenetskaya, O.V.; Vlasov, D.Y. Iron oxalate humboldtine crystallization by fungus *Aspergillus niger*. *Crystals* **2021**, *11*, 1591. [CrossRef]
40. Frank-Kamenetskaya, O.V.; Zelenskaya, M.S.; Izatulina, A.R.; Gurzhiy, V.V.; Rusakov, A.V.; Vlasov, D.Y. Oxalate formation by *Aspergillus niger* on manganese ore minerals. *Am. Mineral.* **2022**, *107*, 100–109. [CrossRef]
41. Available online: www.mindat.org (accessed on 28 January 2023).
42. Sarret, G.; Manceau, A.; Cuny, D.; Haluwyn van, C.; Deruelle, S.; Hazemann, J.-L.; Soldo, I.; Eybert-Berard, L.; Menthonnex, J.-J. Mechanisms of lichen resistance to metallic pollution. *Environ. Sci. Technol.* **1998**, *32*, 3325–3330. [CrossRef]

**Disclaimer/Publisher's Note:** The statements, opinions and data contained in all publications are solely those of the individual author(s) and contributor(s) and not of MDPI and/or the editor(s). MDPI and/or the editor(s) disclaim responsibility for any injury to people or property resulting from any ideas, methods, instructions or products referred to in the content.